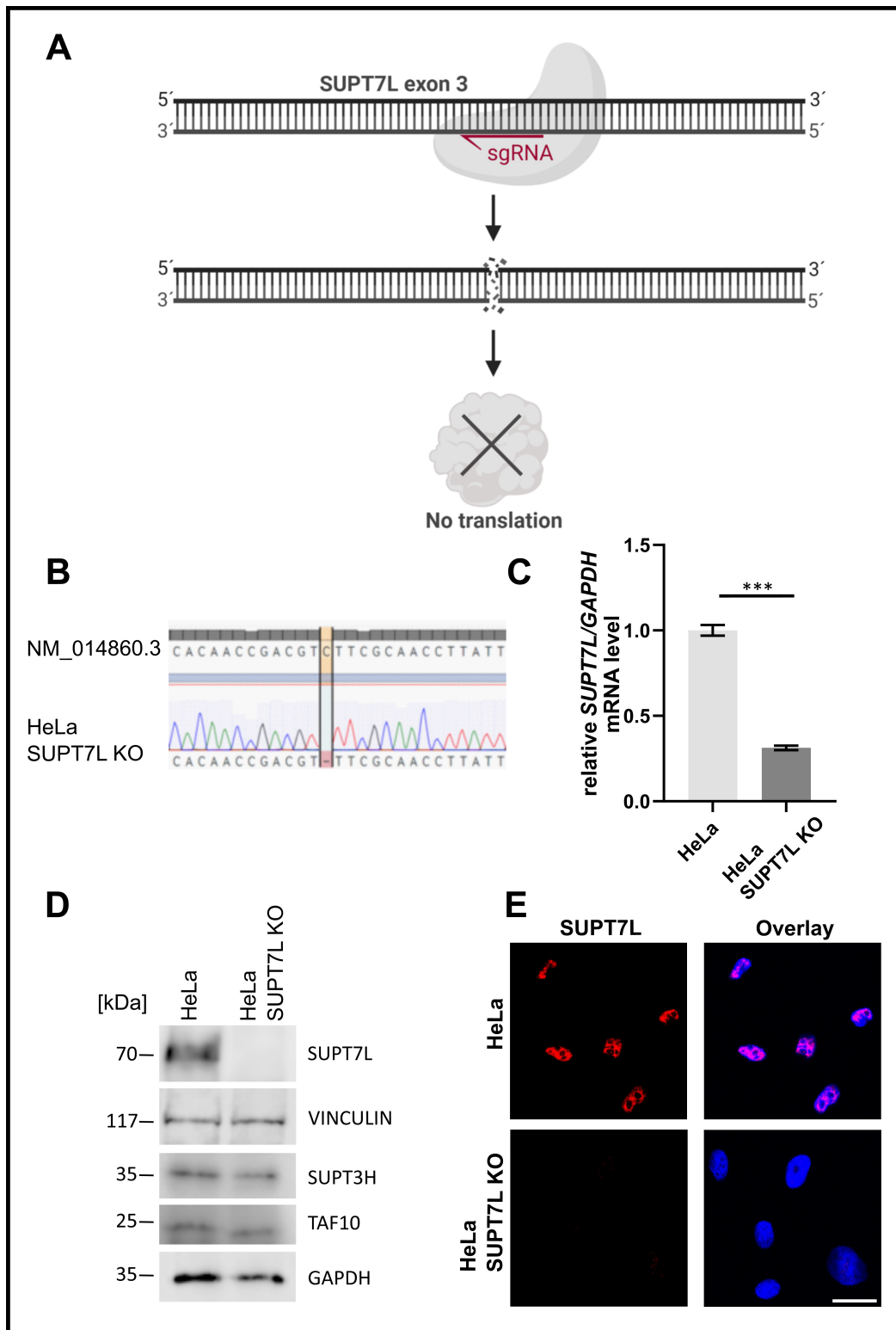


Loss-of-function variants affecting the STAGA complex component *SUPT7L* cause a developmental disorder with generalized lipodystrophy

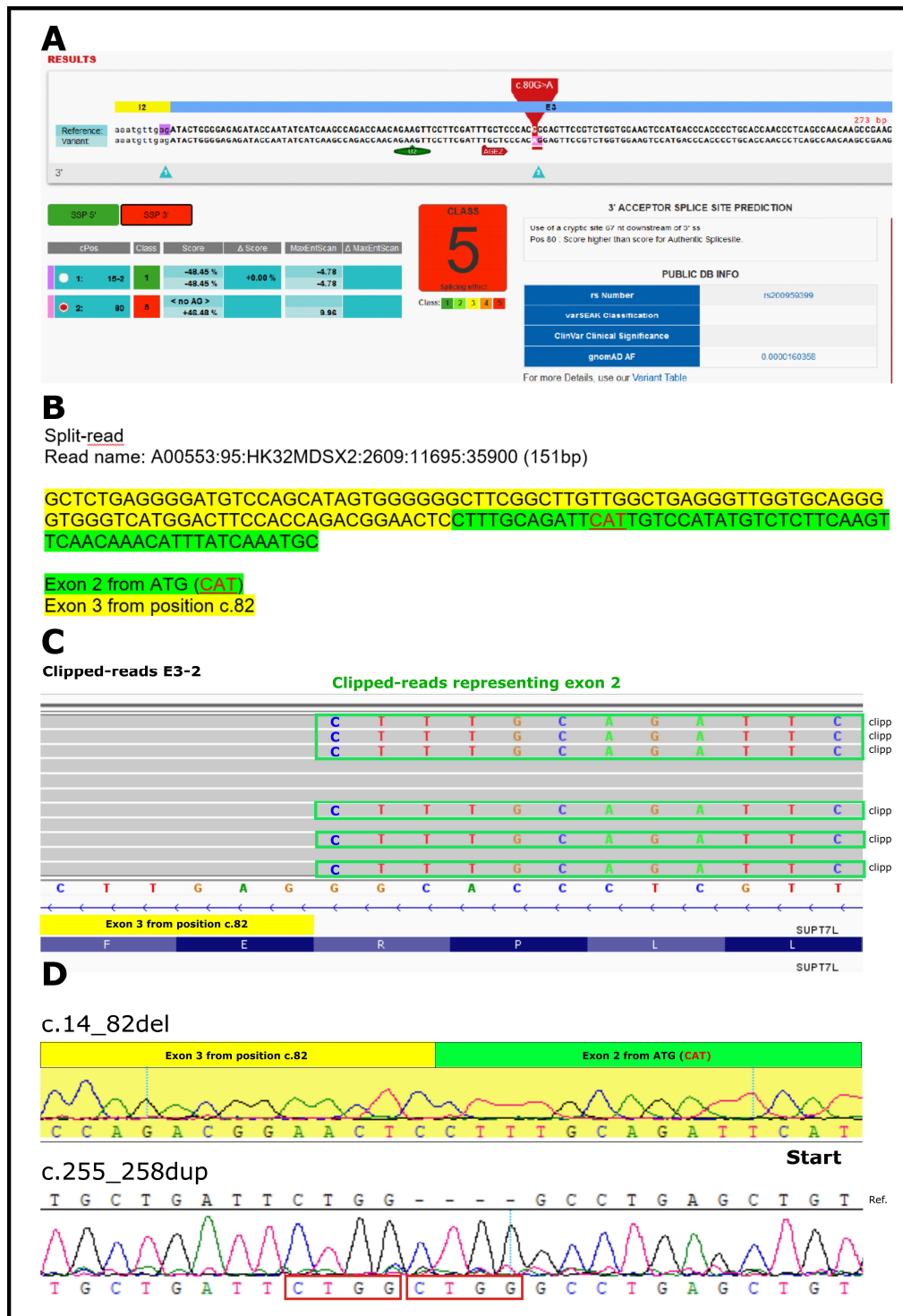
Johannes Kopp, Leonard A. Koch, Hristiana Lyubenova, Oliver Kuchler, Manuel Holtgrewe, Andranik Ivanov, Christele Dubourg, Erika Launay, Sebastian Brachs, Stefan Mundlos, Nadja Ehmke, Dominik Seelow, Mélanie Fradin, Uwe Kornak, Björn Fischer-Zirnsak

Corresponding author: Björn Fischer-Zirnsak PhD,
Charité – Universitätsmedizin Berlin, corporate member of Freie Universität Berlin and Humboldt Universität zu Berlin, Institute
of Medical Genetics and Human Genetics, 13353 Berlin, Germany.
E-mail: bjoern.fischer@charite.de

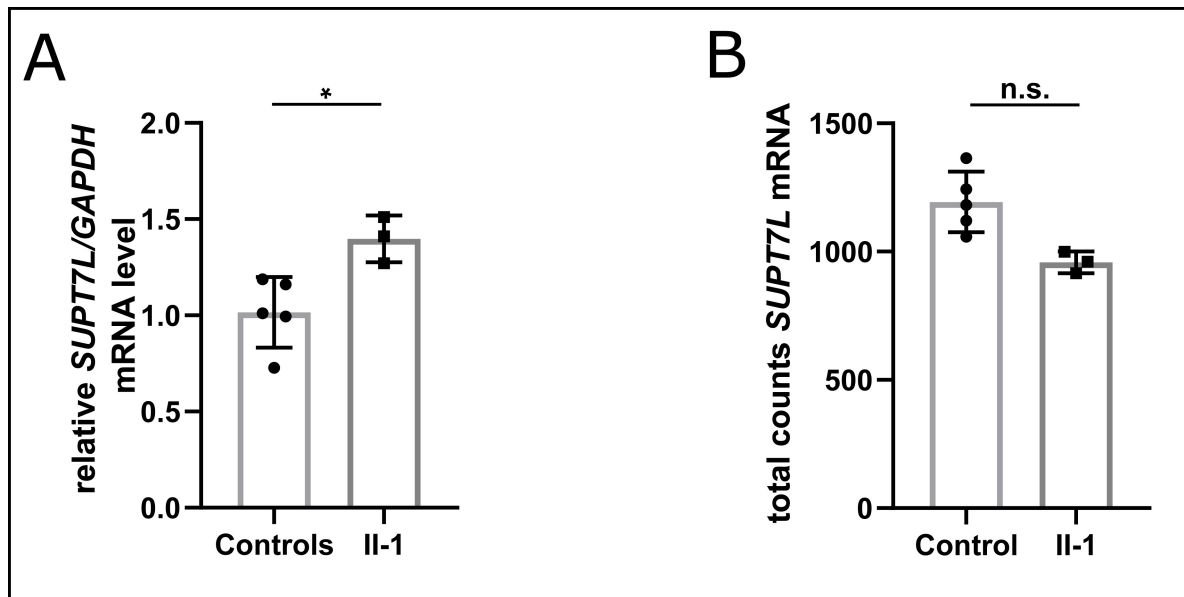
Supplementary Figures 1-10



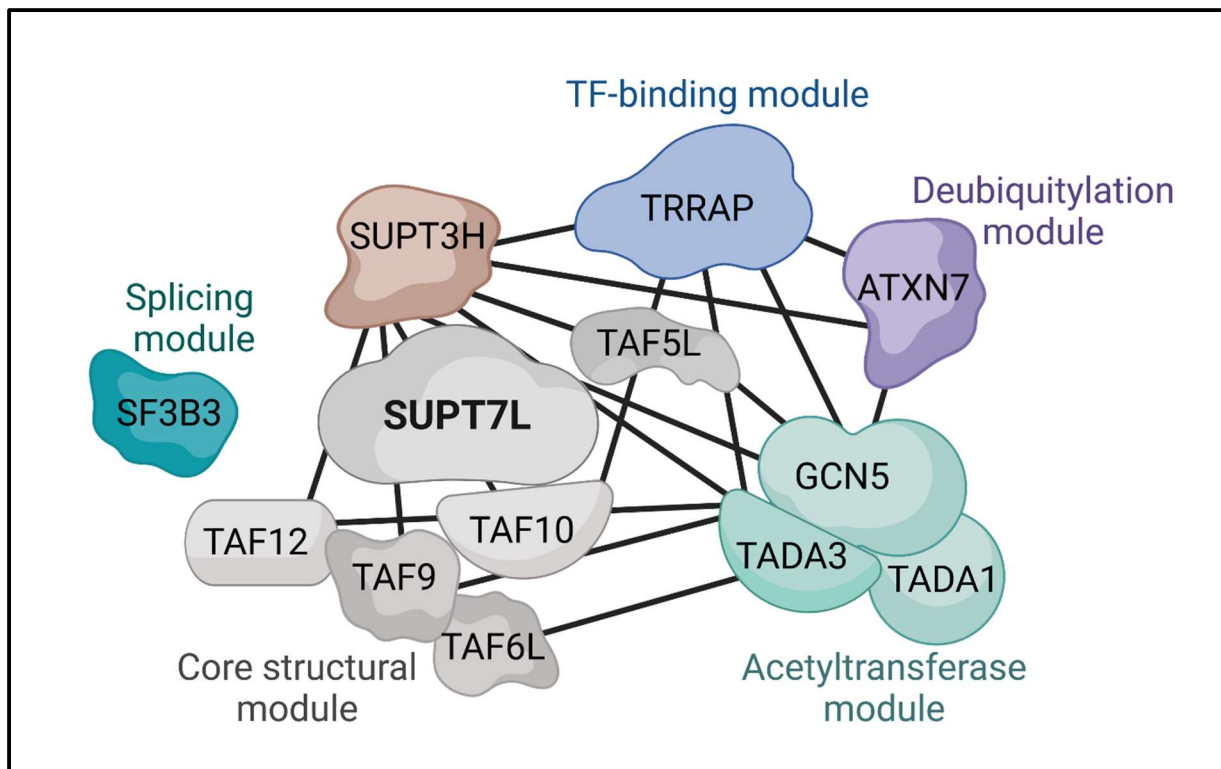
Supplemental Figure 1: **A** Schematic illustration of SUPT7L knockout in HeLa cells using CRISPR/Cas9. SUPT7L-specific sgRNA, binding in exon 3, was designed. **B** Sanger sequencing of exon 3 in the SUPT7L-KO HeLa clone showed the following variant c.226Cdel. **C** Quantitative RT-PCR for SUPT7L was performed in both HeLa WT and SUPT7L-KO cells. Students T-test: $P^{**}<0.01$; $P^{***}<0.001$. **D** Immunoblot detection of SUPT7L, SUPT3H and TAF10 on lysates of HeLa WT and HeLa SUPT7L KO cells. **E** Immunofluorescence staining of SUPT7L in the nucleus. Representative images of SUPT7L (red) and DAPI (blue) in HeLa WT and HeLa SUPT7L KO cells. Scale: 20 μ m



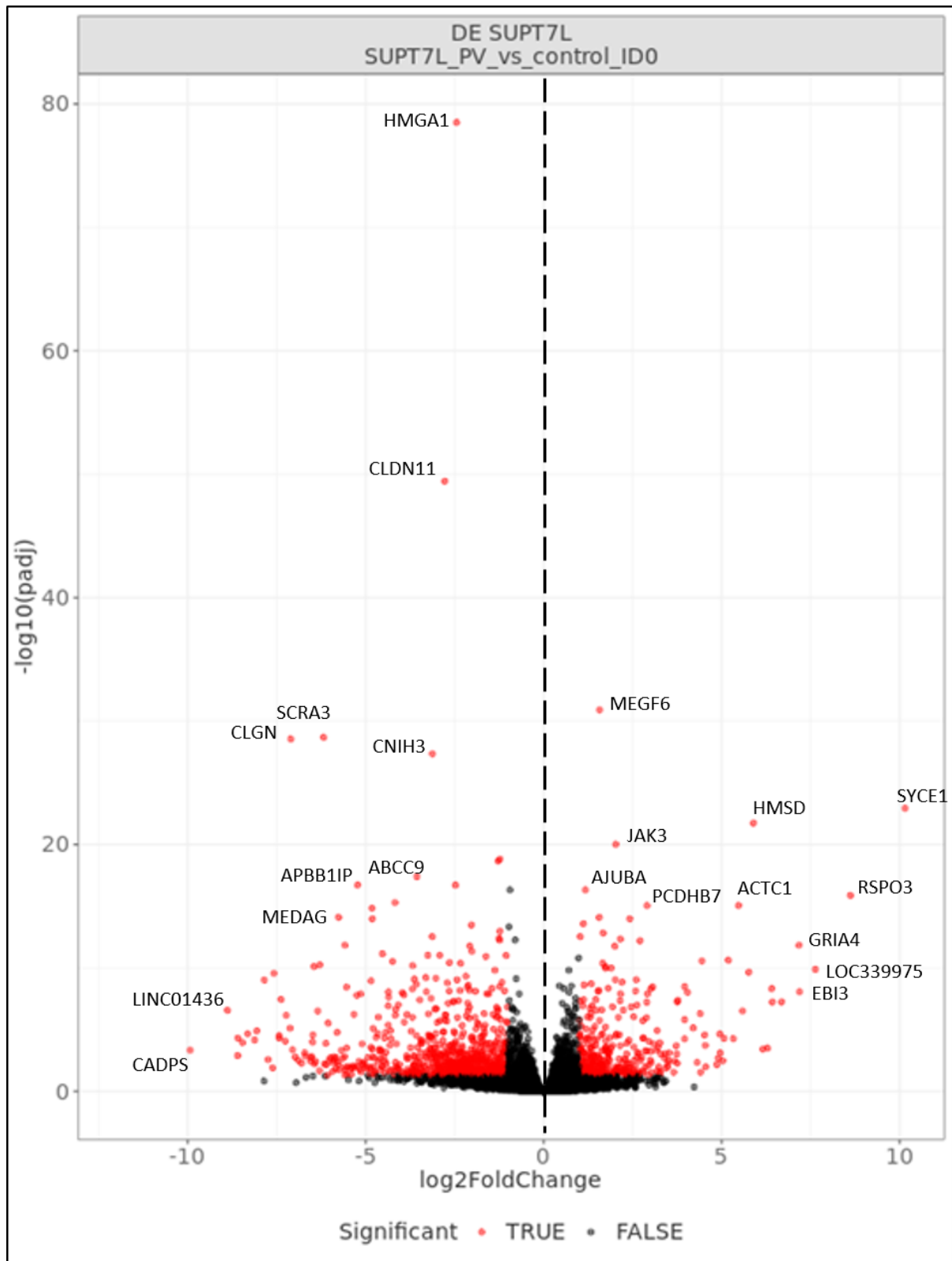
Supplemental Figure 2: **A** VarSEAK classifies the impact of the variant c.80G>A on splicing as a class 5 alteration. Note: all sequences are given as reverse complement to make the directedly comparable to the IGV data. **B** Shows the extracted sequence from a split read representing the aberrant splice event due to the alteration c.80G>A. **C** Shows clipped reads representing the aberrant spliced event due to the alteration c.80G>A. **D** Sanger sequencing of exon 2 and exon 3 on cDNA of II-1. Top: Variant c.80G>A results in an exon truncation due to alternative splicing. The alternative transcript lacks 67 nucleotides and is predicted to results in a frameshift c.14_82del; p.(Arg5fs43*). Bottom: Sanger sequencing of exon 3 on cDNA of II-1. Variant c.255_258dup leads to a frameshift and a premature termination codon after 12 additional codons p.(Asn87Profs*12)



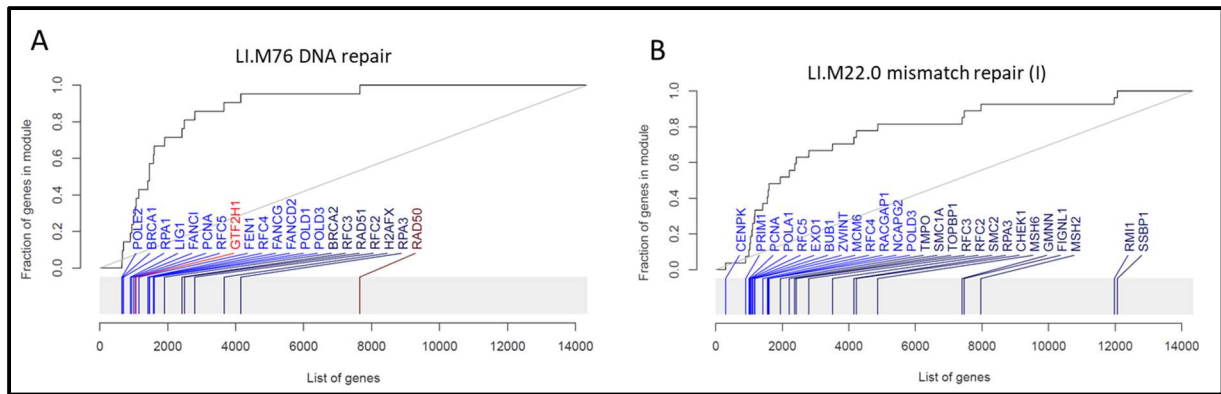
Supplemental Figure 3: Analysis of *SUPT7L* mRNA levels in Fibroblasts of Il-1 compared to 5 unaffected controls. Each Dot represents one sample. **A** Data from quantitative RT-PCR. Students t-test: P < 0.05 . **B** Total counts of *SUPT7L* mRNA reads from transcriptome analysis. P=0.25, n.s. not significant



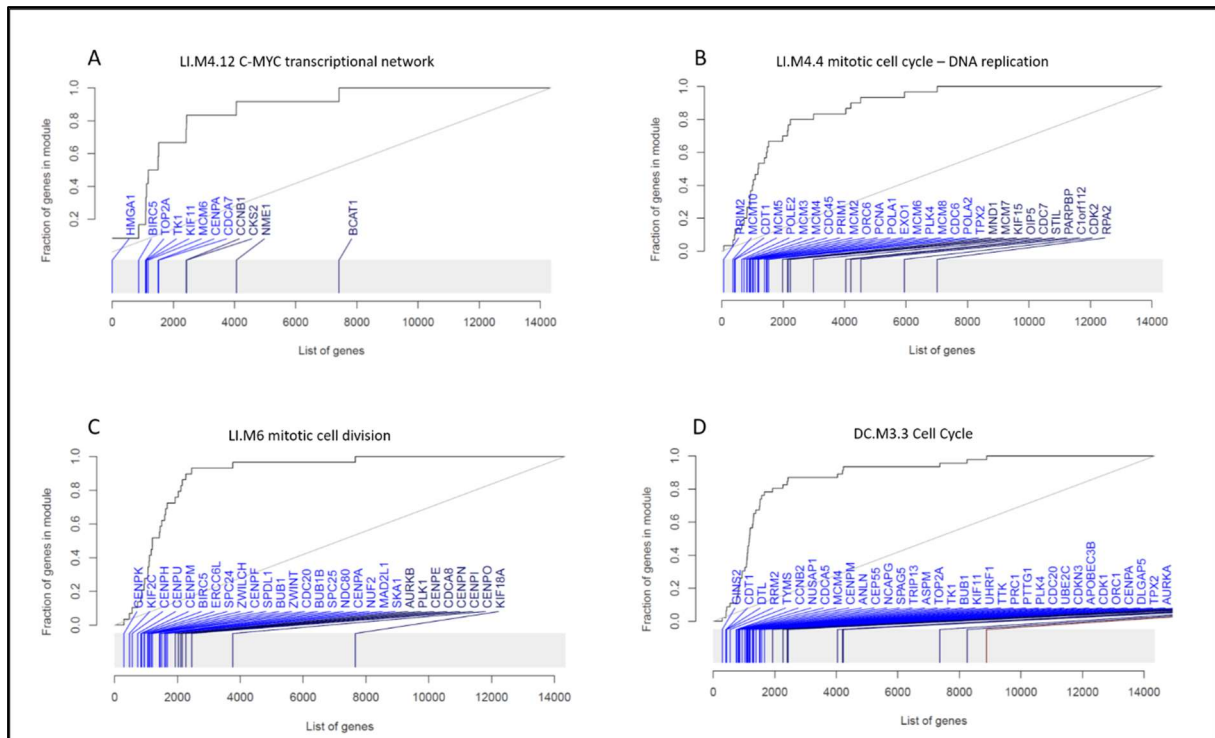
Supplemental Figure 4: Schematic illustration of the STAGA complex with subunits and functional modules. Based and adapted from (Helmlinger and Tora 2017)



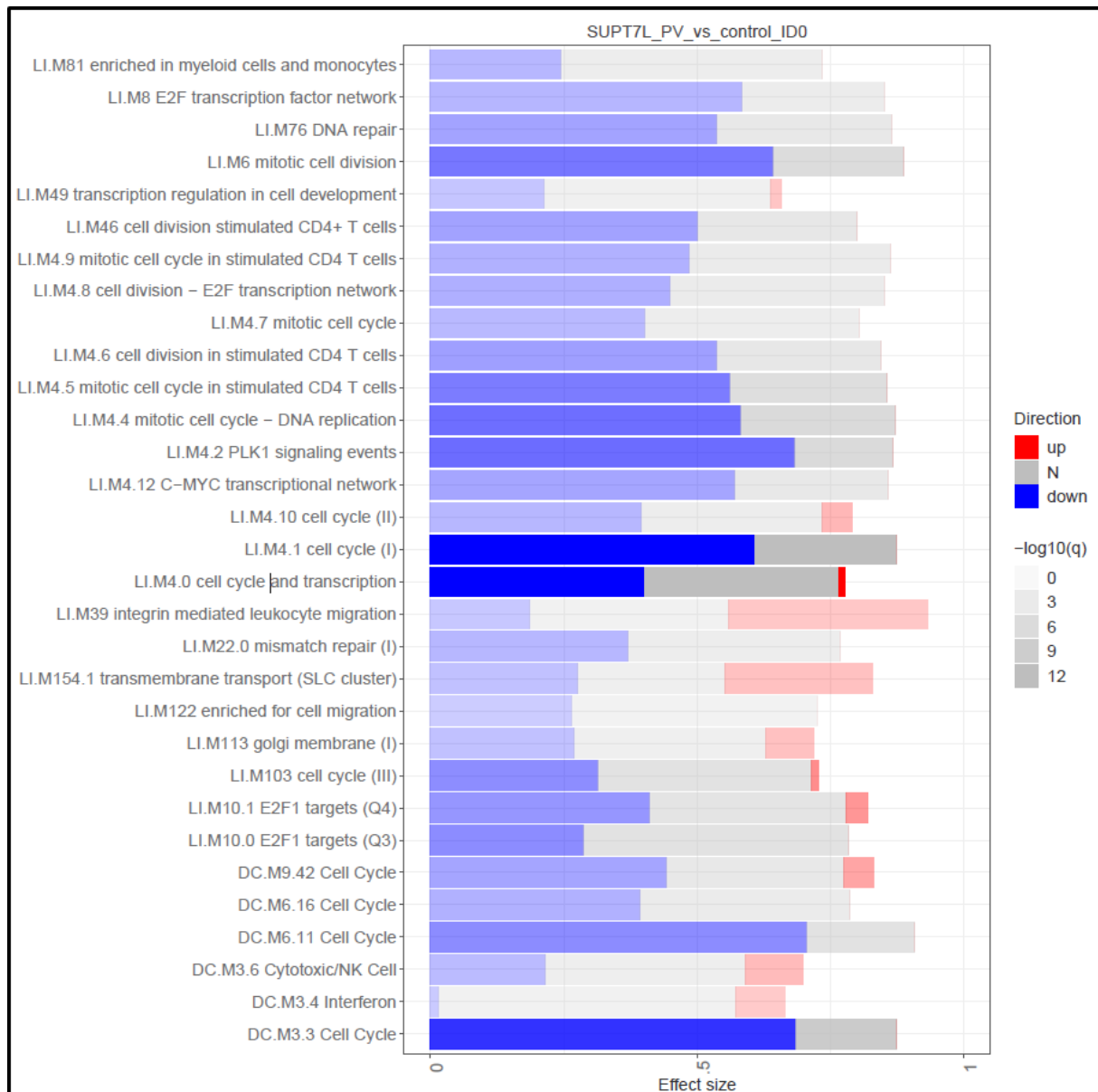
Supplemental Figure 5: Transcriptome sequencing analyses of human Fibroblasts, volcano plot of differential gene expression in Fibroblasts of IL-1 compared to unaffected controls, $p\text{-value} < 0.05$. X-axis shows gene \log_2 fold changes, Y-axis is $-\log_{10}(\text{adj.P-value})$. The most strongly regulated genes in IL-1 are labelled



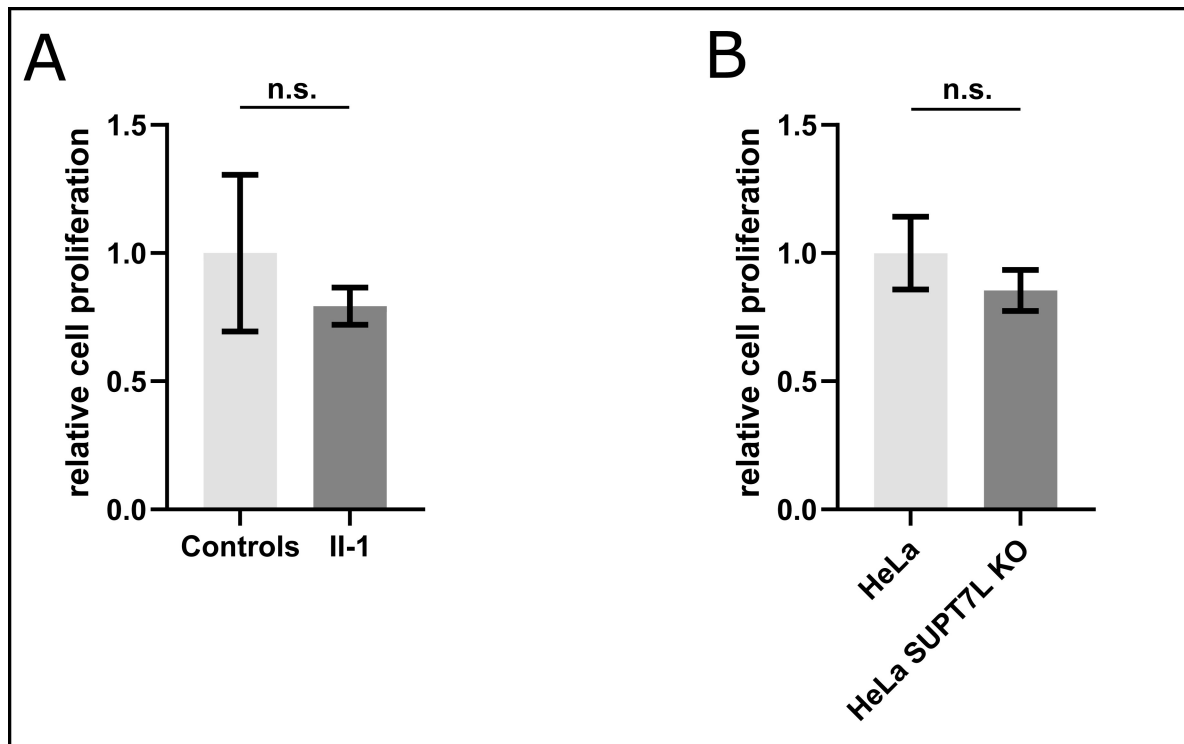
Supplemental Figure 6: Transcriptome sequencing analyses of human Fibroblasts. tmod evidence blot gene sets related to DNA repair. **A** Gene set ID LI.M76, DNA repair, sort order: pval, adj. P value: 0.00034, Effect size (AUC): 0.87. **B** Gene set ID LI.M22.0, mismatch repair (I), sort order: pval, adj. P value: 0.0035, Effect size (AUC): 0.77



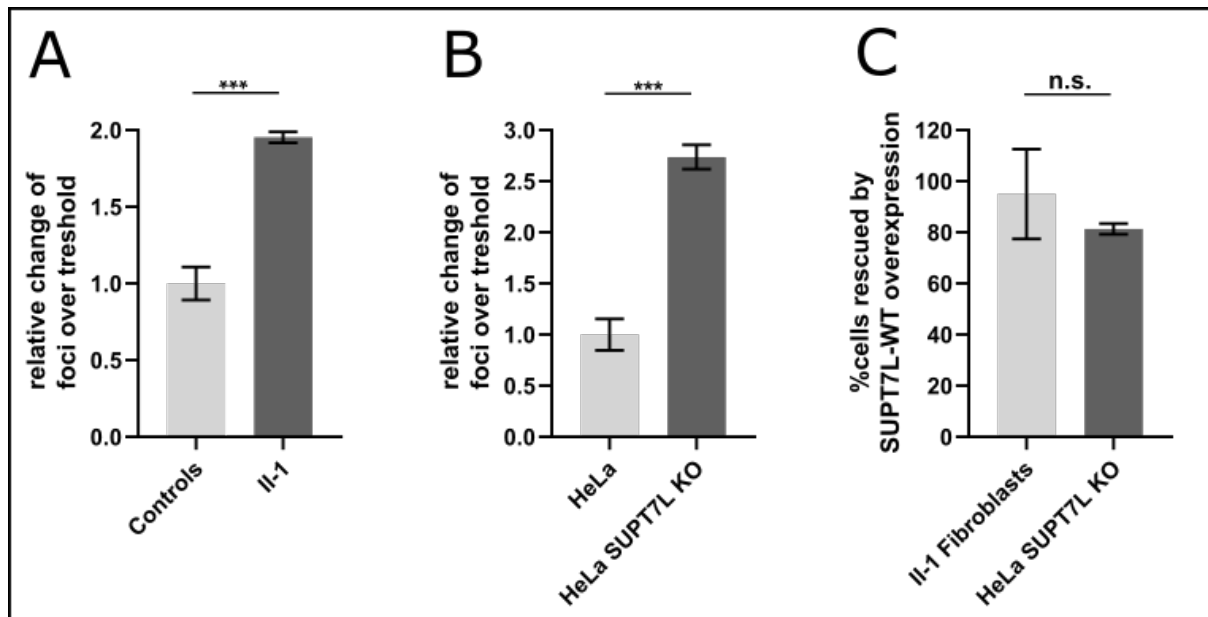
Supplemental Figure 7: Transcriptome sequencing analyses of human Fibroblasts. tmod evidence blot gene sets related to cell cycle and transcription. **A** Gene set ID LI.M4.12, C-MYC transcriptional network, sort order: pval, adj. P value: 0.00043, Effect size (AUC): 0.86. **B** Gene set ID LI.M4.4, mitotic cell cycle - DNA replication, sort order: pval, adj. P value: 5.8e-7, Effect size (AUC): 0.87. **C** Gene set ID LI.M6, mitotic cell division, sort order: pval, adj. P value: 0.0000016, Effect size (AUC): 0.89. **D** Gene set ID DC.M3.3, Cell Cycle, sort order: pval, adj. P value: 4.2e-10, Effect size (AUC): 0.87



Supplemental Figure 8: Transcriptome analysis of fibroblasts from individual II-1 compared to unaffected controls. Shown are all deregulated gene sets from supplementary table 2 with an area under the curve (AUC)>0.65 and $p<0.05$. Up-and down-regulated pathways are shown in red or blue, respectively. Non regulated genes are shown in grey. The effect size represents the AUC, the brightness of the boxes shows the significance



Supplemental Figure 9: Results of WST-1 cell proliferation assay. **A** Relative cell proliferation rate of Fibroblasts of Il-1 compared to 5 unaffected controls after 24h. **B** Relative cell proliferation rate of HeLa *SUPT7L* KO cells compared to HeLa control cells after 24h. Students t-test, ns: not significant



Supplemental Figure 10: Relative change of **DNA damage events**. The relative change in percentage of cells with more than 6 γH2A.X foci was approximately 1.9 times higher in Fibroblasts of IL-1 compared to healthy controls **(A)** and 2.7 times higher in HeLa SUPT7L-KO than in WT cells **(B)**. **C** Percentage Rescue: Quantification of cells with rescued cellular phenotype after transient overexpression of SUPT7L-WT. A significant reduction of percentage of cells with more than 6 γH2A.X foci was observed in patient derived fibroblasts (approximately 95%) and HeLa SUPT7L-KO (approximately 81%) compared to the transfected controls. Students T-test: P***<0.001; n.s.: not significant